

© Copyright 2023, 2024

Jung Ho Chun

Design of De Novo Mimetic Protein of Interleukin-21

Jung Ho Chun

A dissertation

submitted in partial fulfillment of the
requirements for the degree of

Doctor of Philosophy

University of Washington

2023

Reading Committee:

David Baker, Chair

Neil King

Marion Pepper

Program Authorized to Offer Degree:

Biochemistry

University of Washington

Abstract

Design of De Novo Mimetic Protein of Interleukin-21

Jung Ho Chun

Chair of Supervisory Committee:

David Baker

Department of Biochemistry

Interleukin-21 (IL-21) is crucial in coordinating immune cells and has pleiotropic effects in their immune responses. It has established clinical anti-tumor activity in many cancer models. Despite its efficacy, its therapeutic window has been limited due to its systemic toxicity and poor protein engineerability, resulting in the molecule with suboptimal biodistribution and pharmacokinetic properties. In addition, the limited cross-reactivity of human IL-21 in mice complicates the use of animal models to study the toxicity and activity of candidate IL-21 therapeutics. Here, we created de novo IL-21 mimetic proteins that can fully recapitulate its interaction with receptors and the biology of native IL-21 in both humans and mice.

Table of Contents

1. Overall background, challenges, and motivation
2. Design, optimization, and characterization of *de novo* interleukin mimics
 - 2.1. Agonistic mimic of interleukin-21
 - 2.2. Affinity variants and antagonistic mimic of interleukin-21
 - 2.3. Takeaways
3. Acknowledgments
4. Competing interests
5. Reference

List of Figures

Agonistic mimic of interleukin-21

- Fig 2.1.A: The scaffold of the IL-21 mimic is removed for its unstructured regions and extended on helices for ideal helical packing.
- Fig. 2.1.B: Stepwise process for design, screening, optimization, and characterization of IL-21 mimics.
- Fig. 2.1.C: Yeast surface display for binder screening
- Fig. 2.1.D: Hits from initial designs that bind to human IL-21R.
- Fig. 2.1.E: Fluorescence-activated cell sorting of random-mutagenesis library of 21d26.
- Fig. 2.1.F: Site-saturation mutagenesis of 21JC15.
- Fig. 2.1.G: Biolayer interferometry for 21h10's binding against human and murine IL-21 receptors.
- Fig. 2.1.H: Size exclusion chromatography for hydrodynamic sizing.
- Fig. 2.1.I: Circular dichroism for secondary structure and thermal stability.

Affinity variants and antagonistic mimic of interleukin-21

- Fig. 2.2.A: Design of affinity variants of IL-21 mimic.
- Fig. 2.2.B: Characterization of the affinity variants.
- Fig. 2.2.C: Design of 21AT36, an antagonist of IL-21 mimic.
- Fig. 2.2.D: Characterization of the antagonist, 21AT36.

1. Overall background, challenges, and motivation

IL-21, a pivotal member of the γ_c family of cytokines, occupies a central position in regulating a multitude of immune responses and maintaining immune homeostasis. Its mode of action involves the induction of heterodimerization between the IL-21 receptor (IL-21R) and the common γ_c receptor chain, leading to the activation of downstream signaling molecules, particularly phosphorylated STAT proteins. Significantly, IL-21 exhibits pleiotropic effects on various immune cell subsets, encompassing T cells, B cells, natural killer (NK) cells, macrophages, and dendritic cells. Within the context of CD8+ T cells, IL-21 plays a pivotal role in stimulating crucial processes such as cellular proliferation, survival, memory formation, and augmentation of effector functions¹. In the context of B cells, IL-21 serves as a regulator of several fundamental processes, including cell proliferation, differentiation, and the production of immunoglobulins, which collectively contribute to the maintenance of the germinal center reaction².

Furthermore, IL-21 plays a pivotal role in the regulation of natural killer (NK) cells³⁻⁵, influencing their activation, cytotoxicity, and apoptosis. These effects are closely associated with the production of essential cytokines, particularly interferon- γ , which plays a crucial role in mediating anti-tumor⁶⁻⁸ and anti-viral⁹⁻¹¹ effector functions. IL-21's involvement extends to the orchestration of immune responses against infections, cancer, and autoimmune diseases. Consequently, it has garnered substantial attention in clinical research in recent years^{12,13}. Clinical trials involving IL-21 have been conducted across a spectrum of cancer types, including melanoma¹⁴⁻¹⁶, renal cell carcinoma¹⁷, ovarian cancer, and non-Hodgkin's lymphoma. IL-21 has been explored as a standalone therapeutic agent and in combination with other immunotherapeutic modalities, such as immune checkpoint inhibitors and cancer vaccines. The development of IL-21-based cancer therapies represents an exciting frontier in research, holding significant potential for enhancing treatment outcomes for cancer patients. However, the mechanisms underlying IL-21's impact on anti-tumor responses remain incompletely elucidated. Additionally, realizing the full therapeutic potential of native IL-21 has posed challenges due to issues related to its stability and the limited cross-reactivity of human IL-21 in mouse models.

Computational protein design has emerged as a powerful tool for addressing longstanding challenges in protein-based therapeutics. One notable platform in this domain is Rosetta, a specialized computational molecular modeling suite tailored for protein design¹⁸. Rosetta has found widespread application in the creation of de novo proteins with diverse functionalities¹⁸, including peptides¹⁹, therapeutic proteins²⁰⁻²³, biosensors²⁴⁻²⁶, protein cages²⁷⁻²⁹, and vaccines³⁰⁻³². Previously, Rosetta demonstrated its capability in guiding the design of de novo mimetics of IL-2 for cancer therapeutics²⁰. As evidenced by numerous recent instances, computational protein design empowers the development of entirely new proteins

customized to replicate known biological functions or even engender novel reactions previously unobserved in nature^{20,28,33}.

In this study, our objective was to engineer a de novo IL-21 mimetic protein. This protein was designed to recapitulate and enhance the structural features and intermolecular interactions of native IL-21, with an emphasis on enhancing stability while preserving the fundamental biology of native IL-21. Our research showed promising results, showcasing that this IL-21 mimetic protein possesses the potential to be successfully used for therapeutic agents.

2. Design, optimization, and characterization of de novo interleukin mimics

2.1. Agonistic mimic of interleukin-21

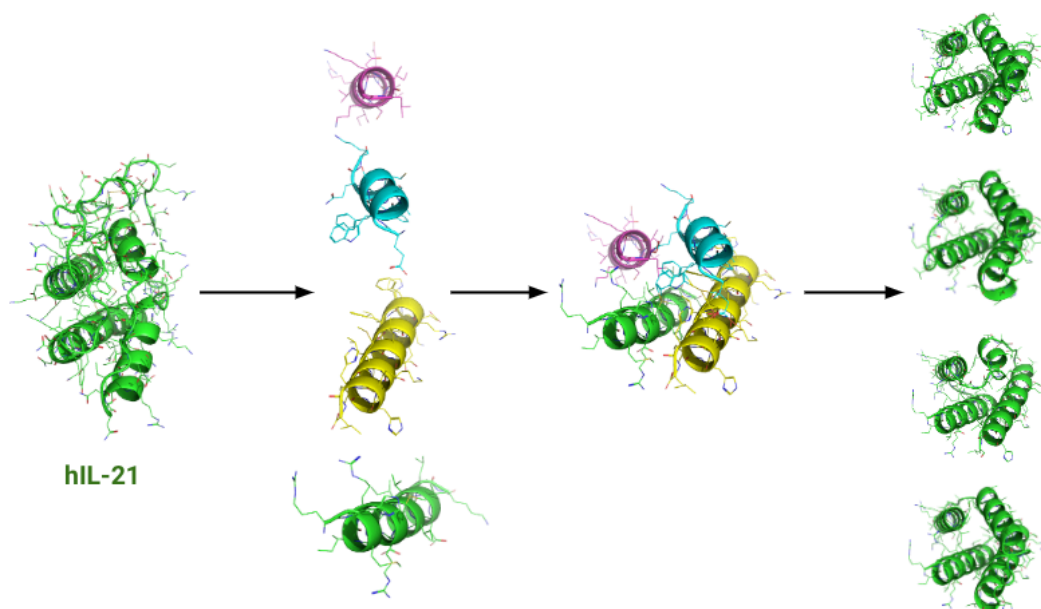


Fig. 2.1.A: The scaffold of the IL-21 mimic is optimized by removing its unstructured regions and extended on helices for **ideal helical packing**. The IL-21 mimics are designed by recapitulating the helical bundle structure of the native human IL-21. Unstructured regions in the hIL-21 are removed, and short helices are extended to accommodate improved intramolecular packing. Some of the native residues conserved from the native human IL-21. Some of its residues are further optimized, as shown.

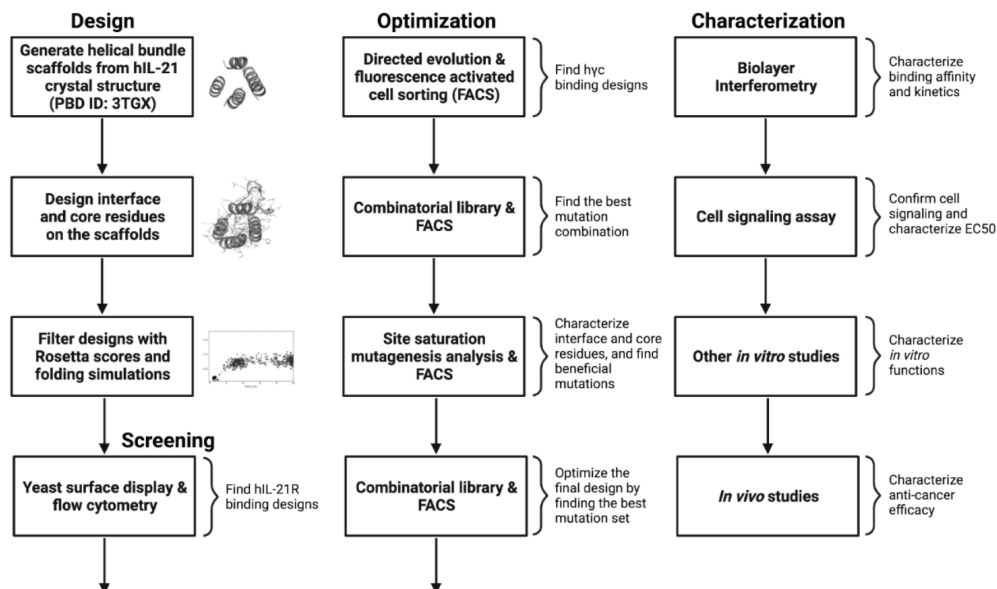


Fig. 2.1.B: Stepwise process for design, screening, optimization, and characterization of IL-21 mimics. The helical bundle scaffolds are generated from the hIL-21 structure, and their residues are designed in the context of hIL-21R (PDB ID: 3TGX). The designs are computationally screened using Rosetta scores and folding simulations. The designs are experimentally screened using yeast surface display with flow cytometry. The optimization processes incorporate directed evolution, site saturation mutagenesis analysis, and combinatorial library screening. Further characterizations use biolayer interferometry, cell signaling assay, other *in vitro* assays, and *in vivo* assays.

We employed a protein design approach to create IL-21 mimics. As the complete structure of the IL-21 receptor complex was unavailable at the time, we used computational modeling. To address the absence of the human γ_c ($h\gamma_c$) structure in the human IL-21/hIL-21R complex³⁴, we incorporated the $h\gamma_c$ chain from the human IL-2 complex³⁵ by using PyRosetta, a computational tool. We generated scaffolds that imitated the helical bundle structure of human IL-21 while enhancing structural stability²⁰. Our optimization efforts included adjusting the lengths of helices, minimizing unstructured regions, and eliminating non-ideal long loops in native human IL-21. Native human IL-21 comprises four helices, with helices A (the first helix from the N-terminus) and C (the third helix) forming an interface to hIL-21R and helix D (the fourth helix) forming an interface to $h\gamma_c$ ^{35,36}. The upper two helices, B and C, are too short to form ideal intramolecular and intermolecular interactions. To improve these helices, we extended them, substituting unstructured regions, including regions between helix pairs A/B and C/D (Fig. 2.1.A). Additionally, we adjusted helices A and D to enhance packing (Fig. 2.1.A). For interface design, we grafted interface residues from hIL-21 onto the scaffolds, designing the remaining residues within the context of hIL-21R using Rosetta. The designed proteins were evaluated and filtered based on Rosetta score metrics and folding trajectories using Fast Forward Folding (Fig. 2.1.B).

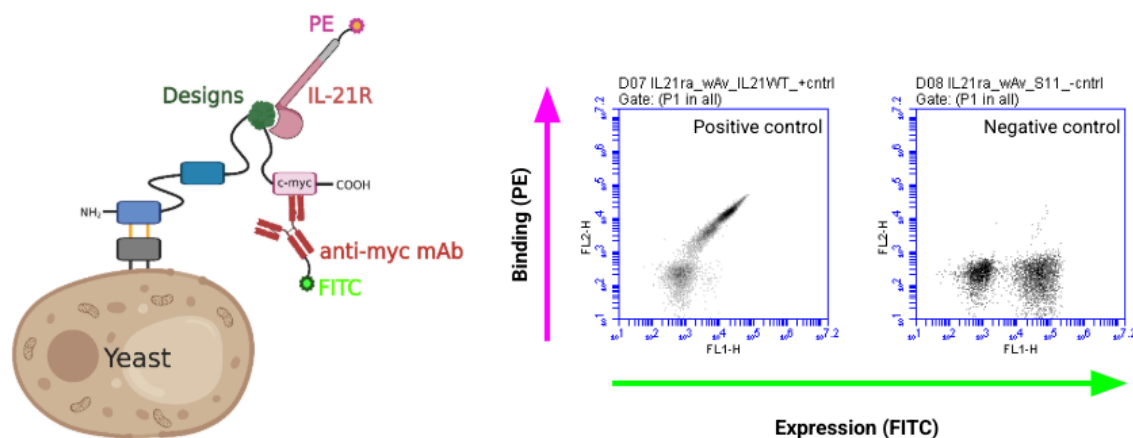


Fig. 2.1.C: Yeast surface display for binder screening. The x-axis represents expression of the protein, labeled as FITC, whereas y-axis represents binding signal, labeled as PE. The cells populate into two groups; the double negative ones are the ones that do not express the design on their cell surface and neither bind to the target receptor. The FITC-positive population is the population that expresses the designed protein on their surface and is able to bind their target receptor, showing diagonal distribution of the population.

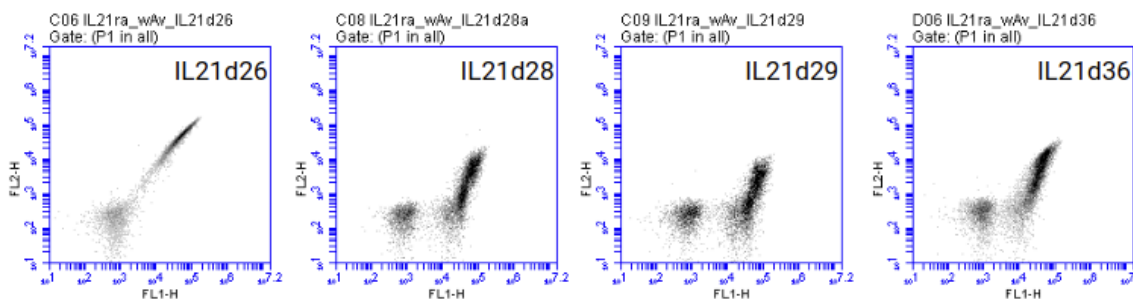


Fig. 2.1.D: Hits from initial designs that bind to human IL-21R. The designs are screened using yeast surface display and tested for receptor binding at 1 μ M.

Four hits were identified out of 36 designs constructed with hIL-21R using yeast surface display as a screening platform (Fig. 2.1.C). These hits bound to hIL-21R but not to $h\gamma_c$ (Fig. 2.1.D). To improve the binding capabilities of our best hit, 21d26, to $h\gamma_c$, we employed directed evolution. We isolated mutants of 21d26 that exhibited $h\gamma_c$ binding in an hIL-21R-dependent manner. One variant, 21JC15, with four mutations (W15C, W49R, Q73H, H99G), displayed the strongest binding affinity. H99G was identified as the critical mutation for acquiring $h\gamma_c$ binding, while the other three mutations enhanced the interface affinity. Incorporating all four mutations into 21d26, we created 21JC15, which exhibited significantly higher affinity than the parent and cross-reactivity between human and murine receptors.

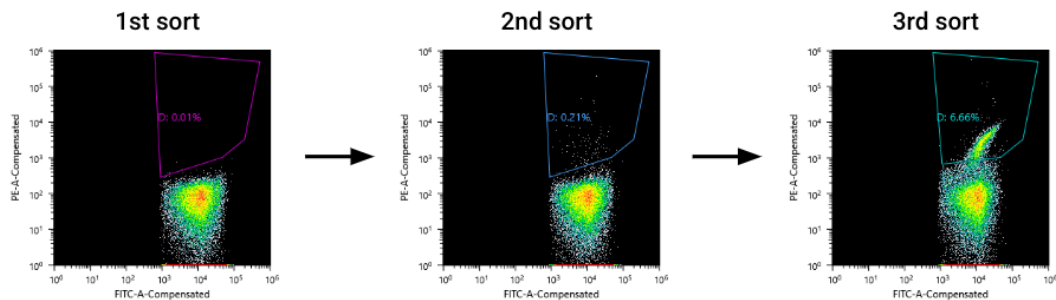


Fig. 2.1.E: Fluorescence-activated cell sorting of random-mutagenesis library of 21d26. The designs are screened using yeast surface display and tested for receptor binding at 1 μ M.

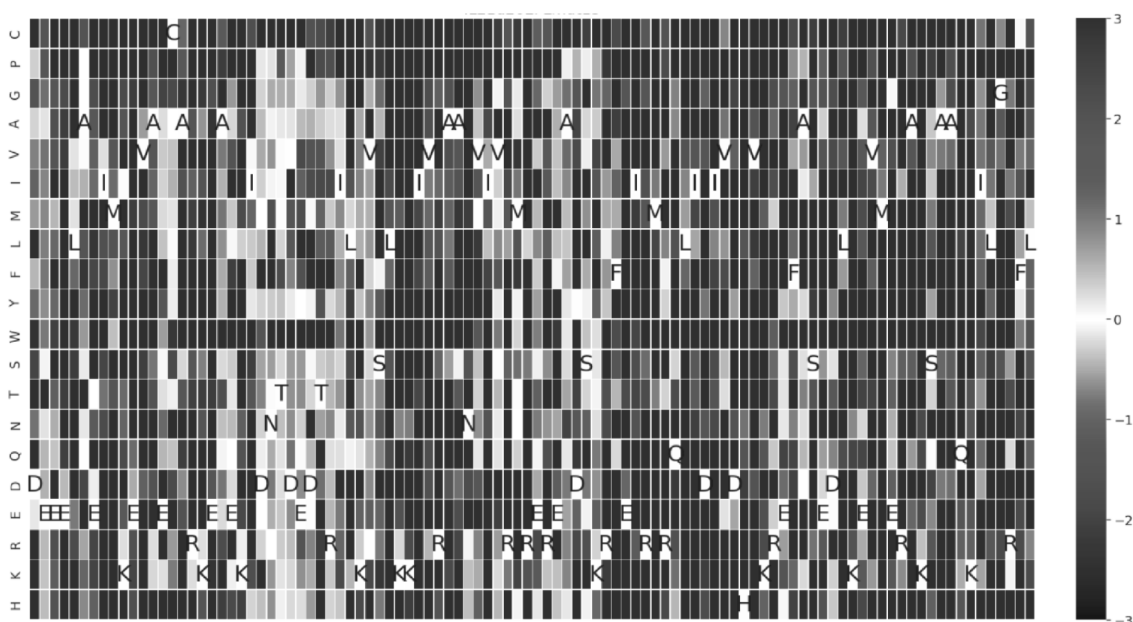


Fig. 2.1.F: Site-saturation mutagenesis of 21JC15.

We used site-saturation mutagenesis to analyze interface residues of 21JC15 for their individual impact on receptor binding affinity (Fig. 2.1.F). Given the combined mutations, we isolated 21h10, a mutant optimized from 21JC15, to exhibit significantly higher affinity than the parent while retaining cross-reactivity between human and murine receptors (Fig. 2.1.G).

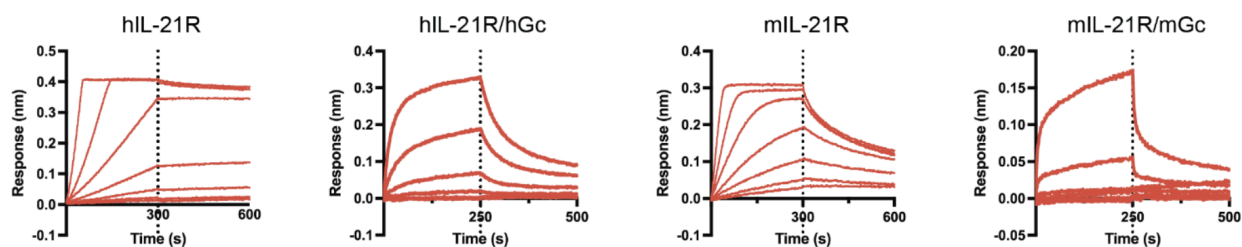


Fig. 2.1.G: Biolayer interferometry for 21h10's binding against human and murine IL-21 receptors. Association and dissociation of 21h10 to human and murine IL-21R and γ_c show concentration-dependent binding curves of 21h10.

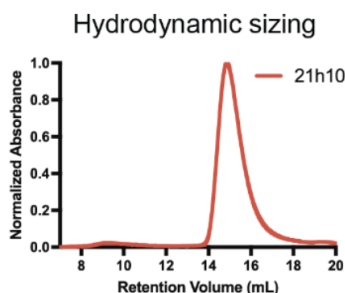


Fig. 2.1.H: Size exclusion chromatography for hydrodynamic sizing. 21h10 exhibits monodispersed distribution when sized through size-exclusion chromatography using Superdex 75 10/300 GL column.

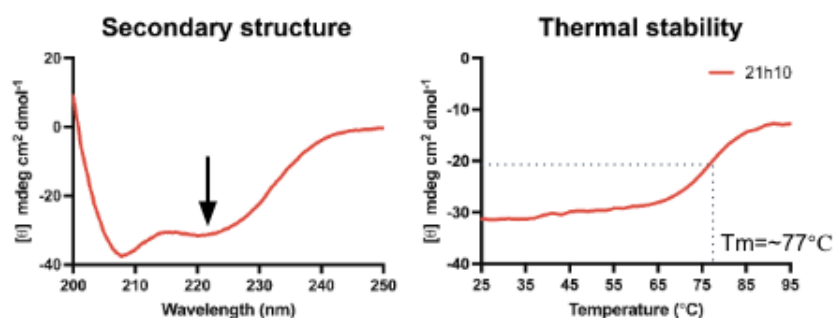


Fig. 2.1.I: Circular dichroism for secondary structure and thermal stability. Wavelength scan from 200 nm to 250 nm confirmed α -helical secondary structure present in 21h10. Thermal melt from 25°C to 95°C with 222 nm scan revealed superior thermal stability of 21h10.

Despite only 44.9% sequence identity to hIL-21 and 23.5% to mL-21³⁷, 21h10 showed cross-reactivity and was tested in various in vitro and in vivo studies. Furthermore, the protein was highly stable and efficiently expressed in *Escherichia coli*. Size-exclusion chromatography confirmed monodispersity in size (Fig. 2.1.H), and circular dichroism analysis confirmed the presence of helical secondary structures and superior thermal stability, holding its helical structure up to 65°C (Fig. 2.1.I).

2.2. Affinity variants and antagonistic mimic of interleukin-21

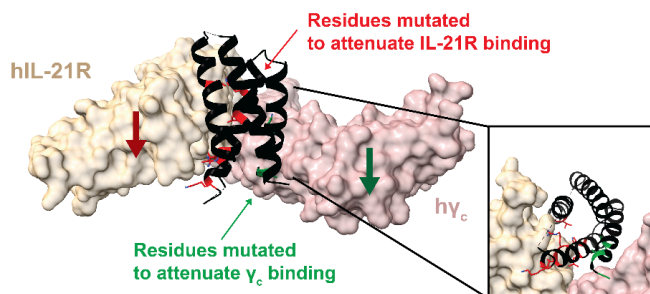


Fig. 2.2.A: Design of affinity variants of IL-21 mimic. Interface residues are mutated (either red or green) to modulate receptor binding affinity to design affinity variants that can bind to the two receptors (IL-21R and γ_c) in a range of affinities.

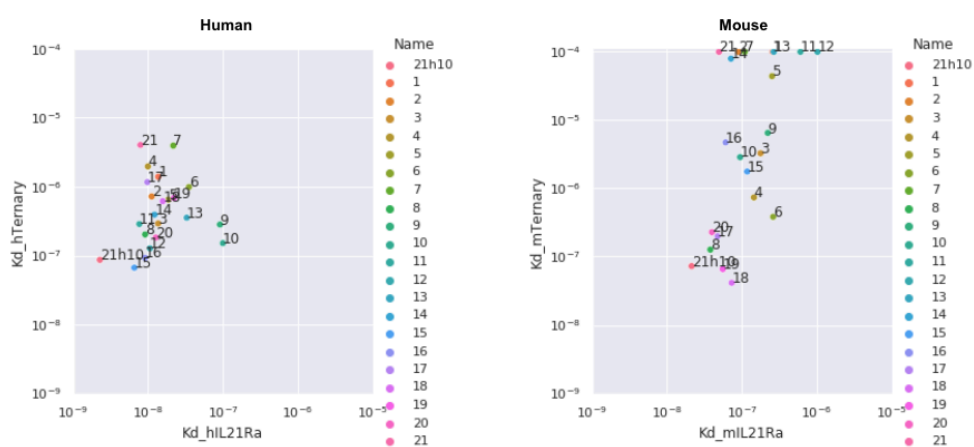


Fig. 2.2.B: Characterization of the affinity variants. Left, human receptor binding affinities of the affinity variants. Right, murine receptor binding affinities of the affinity variants.

Utilizing ProteinMPNN³⁸, we also utilized site-saturation mutagenesis to design affinity-attenuated mutants by weakening affinity from 21h10 (Fig. 2.2.A). A series of variants are acquired by implementing several mutations in the interfaces towards IL-21R and γ_c . The affinity variants with mutations on their receptor binding interfaces show a range of binding affinities to both human and mouse receptors, either IL-21R or IL-21R/ γ_c complex (Fig. 2.2.B). This tuning of the interface affinity is feasible due to robustness of the designed *de novo* proteins with high stability which can withstand mutations. Their binding kinetics to each receptor with association/dissociation rates were measured using biolayer interferometry.

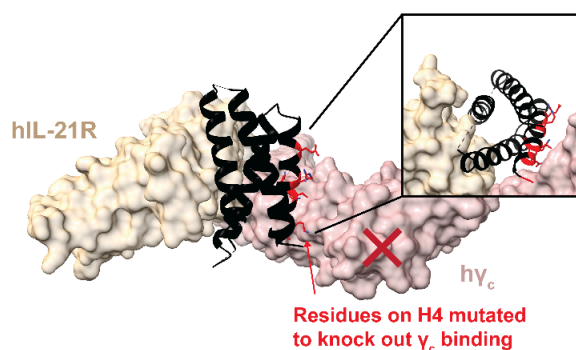


Fig. 2.2.C: Design of 21AT36, an antagonist of IL-21 mimic. Interface residues towards γ_c are mutated (red) to knock out the γ_c binding.

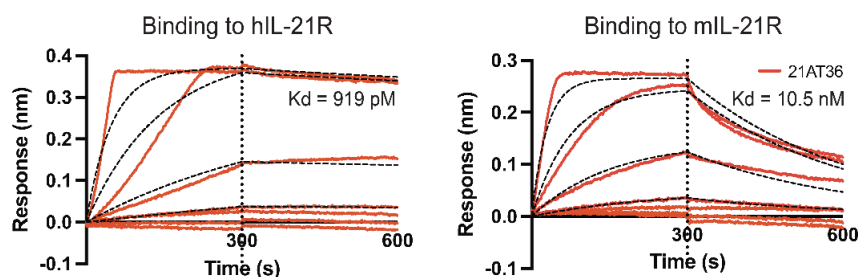


Fig. 2.2.D: Characterization of the antagonist, 21AT36. Association and dissociation of 21AT36 to human and murine IL-21R show concentration-dependent binding curves of 21AT36.

With extensive mutations on the γ_c -interface using ProteinMPNN³⁸, we strategically redesigned the γ_c interface of the most optimized and validated IL-21 mimic, 21h10, to abolish its receptor affinity to achieve antagonistic activity (Fig. 2.2.C). The antagonist hits were screened using yeast surface display, biolayer interferometry, and cell assay to confirm their ability to bind to IL-21R but not γ_c , and antagonism in cells. Their receptor binding affinities to IL-21R are characterized in Fig. 2.2.D.

2.3. Takeaways

Cytokine-based drug development has been a subject of exploration for various clinical applications. However, the engineering of these cytokines for enhanced druggability has been hindered by issues such as poor stability, limited cross-reactivity, and unpredictable behavior of native cytokines. Computational design of de novo proteins has emerged as a promising approach to overcome these limitations by

improving the stability and biochemical properties of native proteins while retaining their binding mechanisms.

Native IL-21 has attracted significant interest as a therapeutic target for conditions like cancer. IL-21 mimics offer a potential avenue to leverage the therapeutic properties of IL-21 while enhancing its molecular stability for optimized engineering. Our computationally designed de novo IL-21 mimic, 21h10, presents several structural and biochemical advantages. First, this mimic demonstrates significantly improved stability, making it highly suitable for further development as a therapeutic agent. Unlike native IL-21, which often faces challenges in expression, 21h10 can be readily produced using *E. coli* and mammalian expression systems. Furthermore, such enhanced stability allows more reliable and consistent data *in vivo* where native IL-21 is impacted by their molecular instability. Third, 21h10 exhibits full cross-reactivity, a feature lacking in native IL-21, and displays comparable receptor binding profiles to its natural counterpart. 21h10 underwent rigorous biochemical and structural validation, confirming its cross-reactivity with human and murine receptors. It recapitulated critical molecular interactions essential for receptor assembly, underscoring the precision of computational protein design.

In summary, the development of 21h10 as a versatile IL-21 mimic with broad immunological applications represents a significant advancement in immunotherapy. The mimic's full cross-reactivity with human and murine systems enables more effective use of animal models for predicting efficacy and toxicity, with full translational possibility. With its numerous advantages, the designed mimics stand as a valuable tool for exploring and harnessing the potential of IL-21-based immunotherapies across diverse disease contexts. Its engineering flexibility opens the door to immunocytokine approaches employing this novel IL-21 mimic and its variants.

3. Acknowledgments

This work was a collaborative effort of multiple teams, including people from **the Institute for Protein Design** and other collaborators within **the University of Washington** and other institutions – National Heart, Lung, and Blood Institute (NHLBI), National Institutes of Health, Seattle Children's Hospital, Harvard University, Dana-Farber Cancer Institute (DFCI), and Stanford University. The successful completion of this project was made possible thanks to the invaluable assistance and support provided by the **Baker Lab**, **King Lab**, and the Institute for Protein Design. **David Baker** played a pivotal role throughout the project, offering invaluable guidance and support. **Neil King's** mentorship during graduate studies and the project are greatly appreciated. I would also like to extend my gratitude to all the members

of both the Baker Lab and the King Lab, who not only fostered a productive working environment but also engaged in valuable discussions that contributed to our progress. Also, I would like to thank all of my collaborators – Warren Leonard, Hao Yuan Kueh, Marion Pepper, Surojit Sarkar, Vandana Kalia, K. Christopher Garcia, Mike Dougan, and Stephanie Dougan – for their invaluable contributions, especially **Mike Dougan** and **Stephanie Dougan**.

Doctoral thesis advisors:

- **David Baker**
- **Neil King**

Doctoral thesis committee:

- David Baker (Chair, Reading Committee)
- Neil King (Reading Committee)
- Marion Pepper (Reading Committee)
- David Veessler
- Leonidas Stamatatos (GSR)

The following people contributed to the design, optimization, and engineering of the protein:

- Institute for Protein Design: Alfredo Quijano-Rubio, Brian Coventry, Cassie Bryan, Daniel Silva, Longxing Cao, Inna Goreshnik, Gyu-Rie Lee, Stephanie Berger, Nihal Korkmaz, Umut Ulge
- BIOFAB: Sam Halabiya, Cami Cordray, Aza Allen

The following people contributed to the production and characterization of the protein, *in vitro* and *in vivo* assays:

- Institute for Protein Design: Stacey Gerben, Michelle DeWitt, Tina Nguyen, Analisa Murray, Piper Heine, Lauren Carter
- Dougan Labs at Harvard University & Dana Farber Cancer Institute: **Mike Dougan**, **Stephanie Dougan**, Birkley Lim, Kevin Zhangxu, Michael Walsh, Tavus Atajanova, Megan Hoffman, Rakeeb Kureshi, Samantha Liu
- Leonard Lab at National Heart, Lung, and Blood Institute (NHLBI), National Institutes of Health: Warren Leonard, Rosanne Spolski, Suyasha Roy, Peng Li
- Kueh Lab at the University of Washington: Hao Yuan Kueh, Elisa C. Clark
- Pepper Lab at the University of Washington: Marion Pepper, Laila Shehata
- Kalia and Sarkar Labs at the University of Washington and Seattle Children's Hospital: Surojit Sarkar, Vandana Kalia, Asheema Khanna, Samantha Tower
- Garcia Lab at Stanford University: K. Christopher Garcia, Gita C. Abhiraman, Kevin M. Jude

The following people contributed to this project through their roles in lab management and doctoral program administration:

- Institute for Protein Design: Lynda Stuart, Lance Stewart, Kristina Herrera, Ratika Krishnamurty, Luki Goldschmidt, Patrick Vecchiato, Kandise VanWormer, Hernan Nunez-Ortega
- Biological Physics, Structure, and Design Ph.D. program and Department of Biochemistry: Erin Kirschner, Chip Asbury, Kelly Lee

The following sources funded this work:

- The National Cancer Institute (R01CA240339)
- The National Institute of Allergy and Infectious Disease (R01AI160052)
- The Washington Research Foundation and Translational Research Fund
- The Open Philanthropy Project Improving Protein Design Fund
- The Audacious Project at the Institute for Protein Design

4. Competing interests

J.C. is one of the co-inventors on a patent application (49605.01US1; 49605.02WO2), which incorporates discoveries described in this thesis. UW FIDS Disclosure #D250035 CoMotion #54400A.

5. Reference

1. Li, Y. & Yee, C. IL-21 mediated Foxp3 suppression leads to enhanced generation of antigen-specific CD8⁺ cytotoxic T lymphocytes. *Blood* **111**, 229–235 (2008).
2. Ozaki, K. *et al.* A critical role for IL-21 in regulating immunoglobulin production. *Science* **298**, 1630–1634 (2002).
3. Brady, J., Hayakawa, Y., Smyth, M. J. & Nutt, S. L. IL-21 induces the functional maturation of murine NK cells. *J. Immunol.* **172**, 2048–2058 (2004).
4. Skak, K., Frederiksen, K. S. & Lundsgaard, D. Interleukin-21 activates human natural killer cells and modulates their surface receptor expression. *Immunology* **123**, 575–583 (2008).
5. Kasaian, M. T. *et al.* IL-21 limits NK cell responses and promotes antigen-specific T cell activation: a mediator of the transition from innate to adaptive immunity. *Immunity* **16**, 559–569 (2002).
6. McMichael, E. L. *et al.* IL-21 Enhances Natural Killer Cell Response to Cetuximab-Coated Pancreatic Tumor Cells. *Clin. Cancer Res.* **23**, 489–502 (2017).
7. Bhatt, S. *et al.* Direct and immune-mediated cytotoxicity of interleukin-21 contributes to antitumor effects in mantle cell lymphoma. *Blood* **126**, 1555–1564 (2015).

8. Gowda, A. *et al.* IL-21 mediates apoptosis through up-regulation of the BH3 family member BIM and enhances both direct and antibody-dependent cellular cytotoxicity in primary chronic lymphocytic leukemia cells in vitro. *Blood* **111**, 4723–4730 (2008).
9. Elsaesser, H., Sauer, K. & Brooks, D. G. IL-21 is required to control chronic viral infection. *Science* **324**, 1569–1572 (2009).
10. Yi, J. S., Du, M. & Zajac, A. J. A vital role for interleukin-21 in the control of a chronic viral infection. *Science* **324**, 1572–1576 (2009).
11. Schmitz, I. *et al.* IL-21 restricts virus-driven Treg cell expansion in chronic LCMV infection. *PLoS Pathog.* **9**, e1003362 (2013).
12. Hashmi, M. H. & Van Veldhuizen, P. J. Interleukin-21: updated review of Phase I and II clinical trials in metastatic renal cell carcinoma, metastatic melanoma and relapsed/refractory indolent non-Hodgkin's lymphoma. *Expert Opin. Biol. Ther.* **10**, 807–817 (2010).
13. Vasu, S. *et al.* A Phase I Clinical Trial Testing the Safety of IL-21-Expanded, Off-the-Shelf, Third-Party Natural Killer Cells for Relapsed/Refractory Acute Myeloid Leukemia and Myelodysplastic Syndrome. *Blood* **136**, 44–44 (2020).
14. Petrella, T. M. *et al.* Interleukin-21 has activity in patients with metastatic melanoma: a phase II study. *J. Clin. Oncol.* **30**, 3396–3401 (2012).
15. Petrella, T. M. *et al.* Final efficacy results of NCIC CTG IND.202: A randomized phase II study of recombinant interleukin-21 (rIL21) in patients with recurrent or metastatic melanoma (MM). *J. Clin. Oncol.* (2013) doi:10.1200/jco.2013.31.15_suppl.9032.
16. Coquet, J. M., Skak, K., Davis, I. D., Smyth, M. J. & Godfrey, D. I. IL-21 Modulates Activation of NKT Cells in Patients with Stage IV Malignant Melanoma. *Clin Transl Immunology* **2**, e6 (2013).
17. Bhatia, S. *et al.* Recombinant interleukin-21 plus sorafenib for metastatic renal cell carcinoma: a phase 1/2 study. *J Immunother Cancer* **2**, 2 (2014).
18. Leman, J. K. *et al.* Macromolecular modeling and design in Rosetta: recent methods and frameworks. *Nat. Methods* (2020) doi:10.1038/s41592-020-0848-2.
19. Hosseinzadeh, P. *et al.* Comprehensive computational design of ordered peptide macrocycles. *Science* **358**, 1461–1466 (2017).
20. Silva, D.-A. *et al.* De novo design of potent and selective mimics of IL-2 and IL-15. *Nature* **565**, 186–191 (2019).
21. Silva, D.-A., Stewart, L., Lam, K.-H., Jin, R. & Baker, D. Structures and disulfide cross-linking of de novo designed therapeutic mini-proteins. *FEBS J.* **285**, 1783–1785 (2018).
22. Chevalier, A. *et al.* Massively parallel de novo protein design for targeted therapeutics. *Nature* **550**, 74–79 (2017).
23. Berger, S. *et al.* Computationally designed high specificity inhibitors delineate the roles of BCL2 family proteins in cancer.

- Elife* **5**, (2016).
24. Langan, R. A. *et al.* De novo design of bioactive protein switches. *Nature* **572**, 205–210 (2019).
 25. Chen, Z. *et al.* Programmable design of orthogonal protein heterodimers. *Nature* **565**, 106–111 (2019).
 26. Jester, B. W., Tinberg, C. E., Rich, M. S., Baker, D. & Fields, S. Engineered Biosensors from Dimeric Ligand-Binding Domains. *ACS Synth. Biol.* **7**, 2457–2467 (2018).
 27. Cannon, K. A. *et al.* Design and structure of two new protein cages illustrate successes and ongoing challenges in protein engineering. *Protein Sci.* **29**, 919–929 (2020).
 28. Bale, J. B. *et al.* Accurate design of megadalton-scale two-component icosahedral protein complexes. *Science* **353**, 389–394 (2016).
 29. Hsia, Y. *et al.* Design of a hyperstable 60-subunit protein dodecahedron. [corrected]. *Nature* **535**, 136–139 (2016).
 30. Kanekiyo, M., Ellis, D. & King, N. P. New Vaccine Design and Delivery Technologies. *J. Infect. Dis.* **219**, S88–S96 (2019).
 31. Marcandalli, J. *et al.* Induction of Potent Neutralizing Antibody Responses by a Designed Protein Nanoparticle Vaccine for Respiratory Syncytial Virus. *Cell* **176**, 1420–1431.e17 (2019).
 32. Brouwer, P. J. M. *et al.* Enhancing and shaping the immunogenicity of native-like HIV-1 envelope trimers with a two-component protein nanoparticle. *Nat. Commun.* **10**, 4272 (2019).
 33. Ng, A. H. *et al.* Modular and tunable biological feedback control using a de novo protein switch. *Nature* **572**, 265–269 (2019).
 34. Crystal Structure of Interleukin-21 Receptor (IL-21R) Bound to IL-21 Reveals That Sugar Chain Interacting with WSXWS Motif Is Integral Part of IL-21R. *J. Biol. Chem.* **287**, 9454–9460 (2012).
 35. Stauber, D. J., Debler, E. W., Horton, P. A., Smith, K. A. & Wilson, I. A. Crystal structure of the IL-2 signaling complex: paradigm for a heterotrimeric cytokine receptor. *Proc. Natl. Acad. Sci. U. S. A.* **103**, 2788–2793 (2006).
 36. Abhiraman, G. C. *et al.* A structural blueprint for interleukin-21 signal modulation. *Cell Rep.* **42**, 112657 (2023).
 37. Altschul, S. F., Gish, W., Miller, W., Myers, E. W. & Lipman, D. J. Basic local alignment search tool. *J. Mol. Biol.* **215**, 403–410 (1990).
 38. Dauparas, J. *et al.* Robust deep learning-based protein sequence design using ProteinMPNN. *Science* **378**, 49–56 (2022).